Study on the selection of BLM detector for C-ADS Injector Ⅱ *

REN Guang-Yi(任广益)[1;1)] ZENG Ming(曾鸣)[2;2)] HE Yuan(何源)[3]
LI Yu-Xiong(李裕熊)[1] LI Wei-Min(李为民)[1]

[1] National Synchrotron Radiation Lab, University of Science and Technology of China, Hefei 230029, China
[2] Tsinghua University, Beijing 100084, China
[3] Institute of Modern Physics, Chinese Academy of Sciences, Lanzhou 730000, China

Abstract: The injector of C-ADS (Chinese Accelerator Driven Sub-critical System) project is a high current, fully super-conducting proton accelerator. Meanwhile, a BLM system is indispensable for this facility, especially in low energy segments. This paper presents some basic simulations for 10 MeV proton by Monte Carlo program FLUKA, as well as the distributions on different secondary particles in three aspects: angular, energy spectrum, and current. These results are beneficial to selecting the detector type and its location and determining its dynamic range matching different requirements for both fast and slow beam loss. Furthermore, in this paper the major impact of the background is also analyzed, such as superconducting cavity X radiation and radiation caused by material activation. This work is meaningful in BLM system research.

Key words: C-ADS, FLUKA, BLM

PACS: 24.10.Lx, 29.27.Eg, 41.85.Qg **DOI:** 10.1088/1674-1137/38/11/117004

1 Introduction

The advantages of the Accelerator-Driven System (ADS) have been widely investigated, including the ability of transmuting high-level radioactive waste (HLW). Injector Ⅱ, as a possible front-end of C-ADS linear accelerator, consisting of an ECR ion source, a 2.1 MeV room temperature RFQ at 162.5 MHz and superconducting half wave resonator (HWR) cavities at 162.5 MHz. The sc accelerating section will stimulate the proton from 2.1 MeV to 10 MeV. Injector Ⅱ will operate in cw mode with a high average current of 10 mA [1].

Beam loss monitors (BLMs) are common devices that are used in hadron and lepton accelerators. Depending on accelerator specifics, BLMs could be used just for diagnostics or they could play an essential role in the machine protection system (MPS). Beam loss control is one of the bottlenecks of beam power increase for this high intensity machine. In contrast from the room temperature accelerating section at the front-end of SNS or J-PARC, C-ADS will accelerate the proton by sc section from 2.1 MeV. Moreover, the sc cavity is more sensitive to beam loss than the room-temperature accelerating section. Thus, it is necessary to provide a high level beam loss monitor system. In this paper, studies on radiation field caused by beam loss of C-ADS Injector Ⅱ will be fully discussed.

2 Monte Carlo simulation

2.1 FLUKA code

Detailed analysis of the radiation field of C-ADS Injector Ⅱ presented in this paper has been performed by the latest version of FLUKA Monte Carlo Code (version 2011.2). FLUKA is a well benchmarked general purpose tool for calculations of particle transport and interactions with matters covering an extended range of applications, for example proton and electron accelerator shielding, target design, calorimetry, activation and dosimetry, cosmic ray studies, and radiotherapy [2].

2.2 Interaction between proton and niobium

Protons lose their energy by ionization and atomic excitation while passing through matter, such as niobium. The main formula governing this process is the Bethe-Bloch equation [3]. The proton range and its secondary particles distribution are simulated in this paper hereafter. The average range of the 10 MeV proton in silicon is 667.4 μm [4]. The 10 MeV proton range in niobium could be figured out according to the formula below:

$$\frac{R_{\rm i}}{R_{\rm o}}=\frac{\rho_{\rm o}\sqrt{A_{\rm i}}}{\rho_{\rm i}\sqrt{A_{\rm o}}},$$

Received 9 December 2013
* Supported by XDA03000000
1) E-mail: gyren@mail.ustc.edu.cn
2) E-mail: zengming@tsinghua.edu.cn

where ρ is the density, A means the atomic mass number, and R represents the particle range. Consequently, the average range of the 10 MeV proton in niobium is 330.7 μm. Then, a 10 MeV proton pencil-beam bombarding the niobium target is simulated by FLUKA. The niobium target is a cylinder of 10 cm in diameter and 0.3 cm in thickness. The simulated range of proton is 312.3 μm, which approximates to the estimate based on the formula.

Figure 1 demonstrates the secondary photon angular distribution of different proton incidence angle. The angle is between the particle direction and the cylindrical bottom. The angular distributions for three incidence angles are similar due to the short proton incident range. In conclusion, the distribution of secondary particles is irrelevant to the proton incidence angle when the proton energy is below 10 MeV.

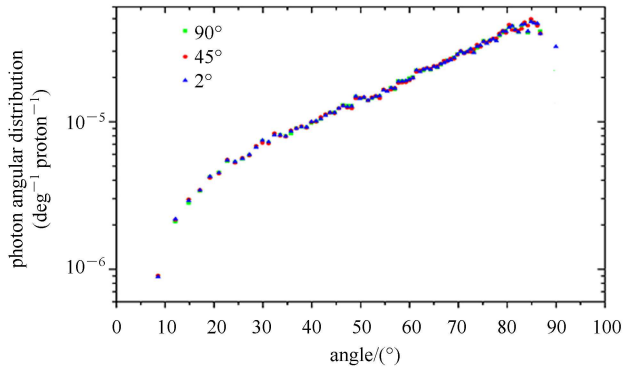

Fig. 1. Photon angular distribution in the case of three different proton incidence angles.

According to Fig. 2, the maximum fluence of photon is performed in the center point. Besides, the fluence distribution of electron and neutron is similar to a photon, which is favorable to electron detection. Because of the very short electron range, the electron could provide proton loss location. However, for photon or neutron, it is difficult for the detector to distinguish where they derive from. On the other hand, a photon or neutron detector will provide a larger detection region.

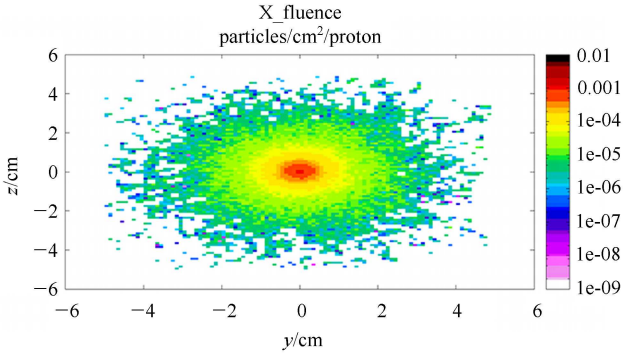

Fig. 2. Photon fluence of cylindrical bottom.

2.3 Proton loss in sc cavity

C-ADS Injector Ⅱ accelerates the proton from 2.1 MeV to 10 MeV by sc cavity, which has a higher accelerating gradient than DTL or CCL and is more sensitive to beam loss for its superconducting state and difficult cleanliness requirements of cavity surface. This is the reason why the sc cavity demands attention and concentration. Since this research is attempting to explore the possibility of a beam loss monitor for the sc cavity, a 10 MeV beam energy, which will produce the most secondary particles, is selected.

Figure 3 depicts the sc HWR cavity and the FLUKA simulation model. In the sc HWR cavity (the upper figure in Fig. 3), the white structure is a niobium cavity and the green one is titanium, which is used as insulation and support. The thicknesses of niobium and titanium are equally 3 mm. The protons pass through the sc cavity by the vacuum part in the center of HWR cavity, with liquid helium filling the gap between niobium and titanium to keep the temperature low.

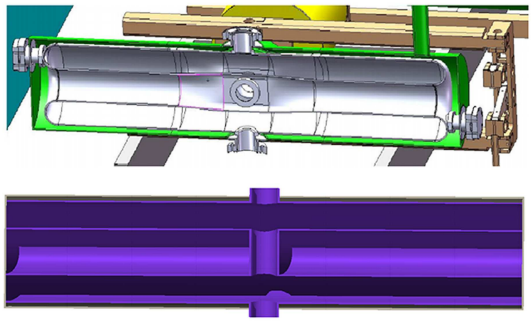

Fig. 3. The upper one is the left view of HWR cavity and the lower one is the top view of the FLUKA model.

Two representative beam loss points are selected and exhibited in Fig. 4. If a detector is assigned on the right side of the cavity, then the detected photon fluence of Fig. 4(b) will be two magnitudes lower than Fig. 4(a). Since the photon of Fig. 4(b) will pass through more materials, such as niobium and liquid helium, it resembles the secondary electron and neutron, which represents that the monitoring of the loss of situation (b) is more arduous than (a) until the detectors could perform rightly in the liquid helium or be placed on both sides.

2.4 Field emission in sc cavity

The sc accelerator may produce a cavity X-ray when it operates on high accelerating gradient. Acknowledgedly, these cavity X-rays are caused by field emission (FE) [5]. The FE is due to quantum tunneling of electrons from microscopic defects on the RF surface,

assisted by the cavity's electric field. Most field emitters occur in the high-electric-field regions near the cavity irises. In the process of accelerating the FE charges (electron mostly), the sped current impacts the cavity walls with diffracting bremsstrahlung X rays.

Since the accelerating voltage is 0.78 MV for the C-ADS sc HWR cavity, the energy of FE electron would be less than 0.78 MeV. If 0.78 MeV electrons hit the sc cavity at the point shown in Fig. 4(a), then the FLUKA simulation result shows that one electron would produce some photons and secondary electrons. The yield of the photon is higher than the situation of proton loss. There is no neutron yielded.

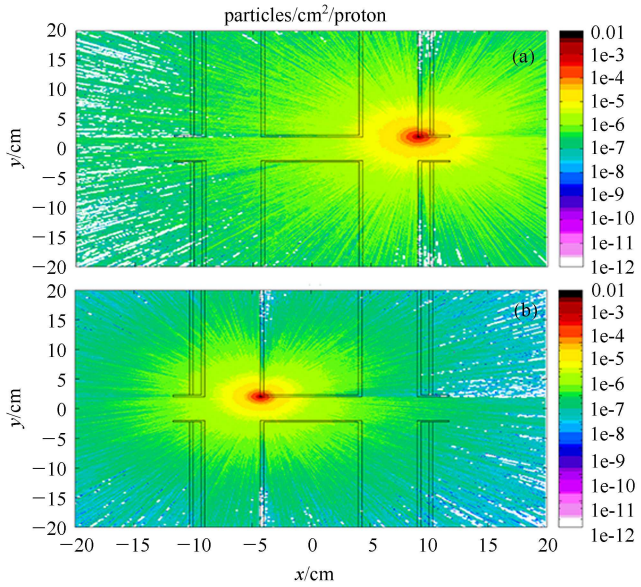

Fig. 4. Two representative beam loss points simulation.

2.5 A simulation of the delayed process

Materials activation is inevitable for any particle accelerator. However, the radiation field of radionuclide should be treated seriously. For simulation purposes, the normal loss that is homogeneously distributed along the HWR cavity inner surface should be taken into consideration. The accepted average beam loss limitation is 1 W/m, representing that 1 cm^2 surface would suffer 1E+8 protons (10 MeV) per second. As indicated by an irradiation simulation executed by FLUKA, the beam current is 1E+8 protons/second after one week-long irradiation.

According to Table 1, the main short half-life radionuclides are Zr(90 m), Nb(94 m), and Mo(93 m), and their activity would reach balancing in two days. Hereafter, the secondary particles could be detected outside the titanium, with some photons, a few electrons and no neutrons. The energy of these photons is below 2.425 MeV and they have a characteristic spectrum.

Table 1. A list of radionuclide (EC=Electron Capture, IT=Isometric Transition).

Z/A	half-life	decay models
Zr(90 m)	809.2 ms	IT
Nb(93 m)	16.13 y	IT
Nb(94)	2.03E+4 y	β-
Nb(94 m)	6.263 m	IT99.5% β-0.5%
Mo(93)	4.0E+3 y	EC
Mo(93 m)	6.85 h	IT99.88% EC0.12%

3 The BLM system

The ultimate goal of a Beam Loss Monitor system is to identify the loss level and, if possible, the loss's location and time structure. Nevertheless, for the C-ADS Injector Ⅱ the primary intention is to protect the machine. Consequently, the BLM should detect the uncontrolled loss as soon as possible and shut down the accelerator immediately.

3.1 Detecting target analysis

Table 2 and Fig. 5 give a complex relationship between the three main beam loss mechanisms and their secondary particles peak yield. Neutron detectors are required because of the sole evidence for proton loss. Meanwhile, the amount of photon yield is the largest, but acquiring the right signal is a challenge assignment to perform. For photon detection, the background would contain the photons caused by normal proton loss, γ-rays by residual radiation, and X-rays by FE sometimes. Since the loss limitation is 1 W/m, there will always be 5.18E+3 photon/second if the FE does not happen. When an uncontrolled loss happens, the beam collapses somewhere. Micro-bunches with length of 6 ns (the specific condition with beam current 10 mA, frequency

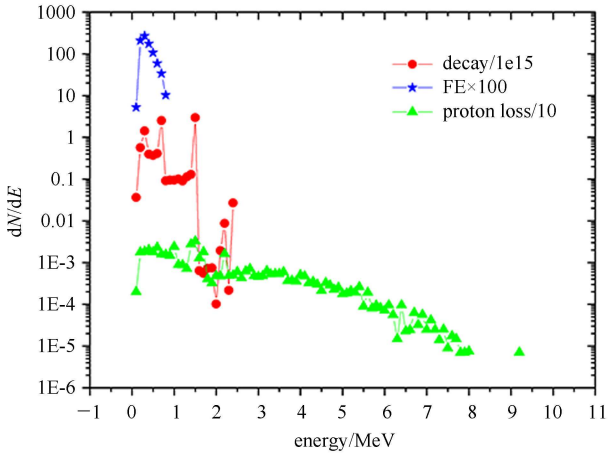

Fig. 5. A photon energy spectrum in three loss mechanisms. (The values of longitudinal axis are adjusted.)

Table 2. Secondary particles peak yield out of sc cavity in 1 cm^2 (s=second, e=electron, p=proton).

source	photon	neutron	electron
proton loss	3.37E-5 /p	1.43e-5 /p	4.34e-7 /p
FE electron	2.26E-3 /e	non	8.42e-7 /e
nuclide decay	1.81E+3 /s	non	little

162.5 MHz) will yield 3.8E+8 protons. One micro-bunch will produce 1.28E+4 photons, which is higher than the background without FE. It is divergent to estimate the influence of FE unless we shield the low energy photons as shown in Fig. 5.

3.2 Detector type analysis

According to the experience of SNS and J-PARC, neutrons and photons are the main detecting particles. In J-PARC, a scintillator and photomultiplier tube loss monitor is provided in the low energy region because of its fast time response [6]. In SNS, neutron detector is useful for machine protection in MEBT and DTL, while the ionization chamber is not sensitive enough at lower energy [7].

The traditional BLM system for proton accelerators mainly consists of ionization chambers and scintillation detectors, such as neutron detectors. This combination is usually not sufficient to protect low-energy high-power proton machines due to:

1) Low radiation level from beam loss,

2) Significant X-ray background near high-gradient superconducting RF cavities, and

3) Poor loss localization with neutron detectors.

Because of the sc cavity, the selection of a beam loss detector is more difficult for the CADS injector. Under such circumstances, an ion chamber is not a good candidate to monitor the beam loss in the cold areas. It is also impossible to place the scintillation detector in the cryomodule because of its large size and low radiation hardness. Diamond detector has high radiation hardness and can be used at low temperature. Consequently, diamond detectors are a promising candidate for BLMs of C-ADS Injector Ⅱ.

In our opinion, a combination of both neutron and gamma detection would be a solution. Neutron detector will be used and placed outside the cryomodule. Diamond detector may be used for gamma detection and should be placed next to the HWR cavity or beam pipe. The performance of the diamond detector should be experimented later.

4 Summary

In this paper, the radiation field caused by beam loss of C-ADS Injector Ⅱ is simulated. The yield of secondary particle is small and the X-ray radiation produced by the RF or sc cavities is relatively large enough. Taking the sc cavity of the CADS injector in to account, special consideration is needed for its BLM detector choice and design. A combination of both neutron and gamma detection would be a solution, such as neutron detector and diamond detector.

The authors would like to express our most sincere thanks to He Yuan (IMP) for his support of this work.

References

1 FU S, FANG S X, LI Z et al. Intense-Beam Issues in CSNS and CADS Accelerators. Proceedings of HB2012. JACoW, 2012. 25

2 Bakkarini F, Battistoni G, Brugger M et al. The Physics of the Fluka Code: Recent Developments. Adv. Space Res., 2007, **40**(9): 1339

3 Zhukov A. Beam Loss Monitors (BLMs): Physics, Simulations and Applications in Accelerators. Proceedings of the 2010 Beam Instrumentation Workshop. Santa Fe, 2010. 553

4 Glenn F. Knoll. Radiation Detection and Measurement. 3rd Ed. John Wily & Sons, 2000

5 Knobloch. Field Emission and Thermal Breakdown in Superconducting Niobium Cavities for Accelerators. IEEE Transactions on Applied Superconductivity, 1999. 1016

6 Igarashi Z, Ikegami M, Miyao T et al. Beam Loss Detected By Scintillation Monitor. Conf. Proc. C110904. 2011, 1257

7 Aleksandrov A. The SNS Beam Diagnostics Experience and Lessons Learned. BIW10, Santa Fe, NM, JACow: 2010. MOIMNB02, 30